

Observation of $B^+ \rightarrow \bar{\Xi}_c^0 \Lambda_c^+$ and Evidence for $B^0 \rightarrow \bar{\Xi}_c^- \Lambda_c^+$

R. Chistov,¹⁰ K. Abe,⁶ I. Adachi,⁶ H. Aihara,⁴¹ Y. Asano,⁴⁴ V. Aulchenko,¹ T. Aushev,¹⁰ S. Bahinipati,³ A. M. Bakich,³⁶ V. Balagura,¹⁰ I. Bedny,¹ U. Bitenc,¹¹ I. Bizjak,¹¹ A. Bondar,¹ A. Bozek,²⁴ M. Bračko,^{6,17,35} J. Brodzicka,²⁴ T. E. Browder,⁵ Y. Chao,²³ A. Chen,²¹ W. T. Chen,²¹ B. G. Cheon,² S.-K. Choi,⁴ Y. Choi,³⁵ Y. K. Choi,³⁵ A. Chuvikov,³² S. Cole,³⁶ J. Dalseno,¹⁸ M. Danilov,¹⁰ M. Dash,⁴⁵ A. Drutskoy,³ S. Eidelman,¹ S. Fratina,¹¹ N. Gabyshev,¹ A. Garmash,³² T. Gershon,⁶ A. Go,²¹ B. Golob,^{16,11} A. Gorišek,¹¹ H. C. Ha,¹³ J. Haba,⁶ K. Hayasaka,¹⁹ H. Hayashii,²⁰ M. Hazumi,⁶ T. Hokuue,¹⁹ Y. Hoshi,³⁹ S. Hou,²¹ W.-S. Hou,²³ T. Iijima,¹⁹ A. Ishikawa,⁶ M. Iwasaki,⁴¹ Y. Iwasaki,⁶ P. Kapusta,²⁴ N. Katayama,⁶ T. Kawasaki,²⁶ H. R. Khan,⁴² H. Kichimi,⁶ H. J. Kim,¹⁴ S. M. Kim,³⁵ K. Kinoshita,³ S. Korpar,^{17,11} P. Krokovny,¹ R. Kulasiri,³ C. C. Kuo,²¹ A. Kuzmin,¹ Y.-J. Kwon,⁴⁶ G. Leder,⁹ T. Lesiak,²⁴ S.-W. Lin,²³ D. Liventsev,¹⁰ J. MacNaughton,⁹ G. Majumder,³⁷ F. Mandl,⁹ T. Matsumoto,⁴³ W. Mitaroff,⁹ H. Miyake,²⁹ H. Miyata,²⁶ Y. Miyazaki,¹⁹ R. Mizuk,¹⁰ J. Mueller,³¹ Y. Nagasaka,⁷ E. Nakano,²⁸ M. Nakao,⁶ S. Nishida,⁶ S. Ogawa,³⁸ T. Ohshima,¹⁹ S. Okuno,¹² S. L. Olsen,⁵ Y. Onuki,²⁶ W. Ostrowicz,²⁴ H. Ozaki,⁶ P. Pakhlov,¹⁰ H. Palka,²⁴ H. Park,¹⁴ K. S. Park,³⁵ L. S. Peak,³⁶ R. Pestotnik,¹¹ L. E. Piilonen,⁴⁵ Y. Sakai,⁶ N. Sato,¹⁹ N. Satoyama,³⁴ T. Schietinger,¹⁵ O. Schneider,¹⁵ K. Senyo,¹⁹ M. E. Sevior,¹⁸ A. Somov,³ R. Stamen,⁶ S. Stanič,²⁷ M. Starič,¹¹ T. Sumiyoshi,⁴³ S. Y. Suzuki,⁶ F. Takasaki,⁶ N. Tamura,²⁶ M. Tanaka,⁶ G. N. Taylor,¹⁸ Y. Teramoto,²⁸ X. C. Tian,³⁰ T. Tsukamoto,⁶ S. Uehara,⁶ T. Uglov,¹⁰ K. Ueno,²³ Y. Unno,⁶ S. Uno,⁶ G. Varner,⁵ K. E. Varvell,³⁶ S. Villa,¹⁵ C. C. Wang,²³ C. H. Wang,²² M.-Z. Wang,²³ E. Won,¹³ Q. L. Xie,⁸ A. Yamaguchi,⁴⁰ Y. Yamashita,²⁵ M. Yamauchi,⁶ C. C. Zhang,⁸ J. Zhang,⁶ L. M. Zhang,³³ Z. P. Zhang,³³ and V. Zhilich¹

(The Belle Collaboration)

¹*Budker Institute of Nuclear Physics, Novosibirsk*

²*Chonnam National University, Kwangju*

³*University of Cincinnati, Cincinnati, Ohio 45221*

⁴*Gyeongsang National University, Chinju*

⁵*University of Hawaii, Honolulu, Hawaii 96822*

⁶*High Energy Accelerator Research Organization (KEK), Tsukuba*

⁷*Hiroshima Institute of Technology, Hiroshima*

⁸*Institute of High Energy Physics, Chinese Academy of Sciences, Beijing*

⁹*Institute of High Energy Physics, Vienna*

¹⁰*Institute for Theoretical and Experimental Physics, Moscow*

¹¹*J. Stefan Institute, Ljubljana*

¹²*Kanagawa University, Yokohama*

¹³*Korea University, Seoul*

¹⁴*Kyungpook National University, Taegu*

¹⁵*Swiss Federal Institute of Technology of Lausanne, EPFL, Lausanne*

¹⁶*University of Ljubljana, Ljubljana*

¹⁷*University of Maribor, Maribor*

¹⁸*University of Melbourne, Victoria*

¹⁹*Nagoya University, Nagoya*

²⁰*Nara Women's University, Nara*

²¹*National Central University, Chung-li*

²²*National United University, Miao Li*

²³*Department of Physics, National Taiwan University, Taipei*

²⁴*H. Niewodniczanski Institute of Nuclear Physics, Krakow*

²⁵*Nippon Dental University, Niigata*

²⁶*Niigata University, Niigata*

²⁷*Nova Gorica Polytechnic, Nova Gorica*

²⁸*Osaka City University, Osaka*

²⁹*Osaka University, Osaka*

³⁰*Peking University, Beijing*

³¹*University of Pittsburgh, Pittsburgh, Pennsylvania 15260*

³²*Princeton University, Princeton, New Jersey 08544*

³³*University of Science and Technology of China, Hefei*

³⁴*Shinshu University, Nagano*

³⁵*Sungkyunkwan University, Suwon*

³⁶*University of Sydney, Sydney NSW*

³⁷*Tata Institute of Fundamental Research, Bombay*

³⁸Toho University, Funabashi

³⁹Tohoku Gakuin University, Tagajo

⁴⁰Tohoku University, Sendai

⁴¹Department of Physics, University of Tokyo, Tokyo

⁴²Tokyo Institute of Technology, Tokyo

⁴³Tokyo Metropolitan University, Tokyo

⁴⁴University of Tsukuba, Tsukuba

⁴⁵Virginia Polytechnic Institute and State University, Blacksburg, Virginia 24061

⁴⁶Yonsei University, Seoul

We report the first observation of the decay $B^+ \rightarrow \Xi_c^0 \Lambda_c^+$ with a significance of 8.7σ and evidence for the decay $B^0 \rightarrow \Xi_c^- \Lambda_c^+$ with a significance of 3.8σ . The product $\mathcal{B}(B^+ \rightarrow \Xi_c^0 \Lambda_c^+) \times \mathcal{B}(\Xi_c^0 \rightarrow \Xi^+ \pi^-)$ is measured to be $(4.8_{-0.9}^{+1.0} \pm 1.1 \pm 1.2) \times 10^{-5}$, and $\mathcal{B}(B^0 \rightarrow \Xi_c^- \Lambda_c^+) \times \mathcal{B}(\Xi_c^- \rightarrow \Xi^+ \pi^- \pi^-)$ is measured to be $(9.3_{-2.8}^{+3.7} \pm 1.9 \pm 2.4) \times 10^{-5}$. The errors are statistical, systematic and the error of the $\Lambda_c^+ \rightarrow p K^- \pi^+$ branching fraction, respectively. The decay $B^+ \rightarrow \Xi_c^0 \Lambda_c^+$ is the first example of a two-body exclusive B^+ decay into two charmed baryons. The data used for this analysis was accumulated at the $\Upsilon(4S)$ resonance, using the Belle detector at the e^+e^- asymmetric-energy collider KEKB. The integrated luminosity of the data sample is equal to 357 fb^{-1} , corresponding to $386 \times 10^6 B\bar{B}$ pairs.

PACS numbers: 13.25.Hw, 14.20.Lq

A number of B -meson decay modes to final states containing baryons have been observed, including $b \rightarrow c\bar{u}d$ decays with either one final-state charmed meson (e.g. $B^0 \rightarrow \bar{D}^0 p \bar{p}$ [1]) or a charmed baryon (e.g. $B^+ \rightarrow \bar{\Lambda}_c^- p \pi^+$ [2]), and charmless baryonic decays [3] that proceed via $b \rightarrow s$ or $b \rightarrow u$ transitions. Two-body baryonic decay modes are found to have lower branching fractions than multi-body modes and, in the latter, near-threshold enhancements are observed in the baryon-pair invariant mass spectra [4]. Some theoretical models attribute these phenomena to baryonic form factors that are large for multi-body modes [5].

Recently, Belle reported examples of baryonic decays that proceed via $b \rightarrow c\bar{c}s$ transitions: $B^- \rightarrow J/\psi \Lambda \bar{p}$ [6] and $B \rightarrow \Lambda_c^+ \bar{\Lambda}_c^- K$ [7]. To date, however, nothing is experimentally known about two-body exclusive B decays to two charmed baryons, which would also proceed through $b \rightarrow c\bar{c}s$ transitions. An example of such a decay is $B^+ \rightarrow \Xi_c^0 \Lambda_c^+$, which would proceed via the quark diagram shown in Fig. 1. This two-body B decay mode, like $B \rightarrow \Lambda_c^+ \bar{\Lambda}_c^- K$, would produce a “wrong-sign” Λ_c^+ , in contrast to all other known B decay modes that only have $\bar{\Lambda}_c^-$ ’s in the final state [8]. Recently the BaBar collaboration has measured the inclusive yield of (wrong-sign) Λ_c^+ ’s from B decays [9]. It was suggested that this type of B decay might be a substantial component of baryonic $b \rightarrow c\bar{c}s$ transitions and could have an important influence on the determination of the charm particle yield per B decay [10].

For exclusive two-body baryonic modes, a theoretical model based on QCD sum rules predicts $\mathcal{B}(B \rightarrow \Xi_c \Lambda_c^+) \sim 10^{-3}$ [11]. Experimental measurements of $B \rightarrow \Xi_c \Lambda_c^+$ test theoretical predictions and provide additional information on the dynamics of two-body baryonic B decays.

In this Letter we report the first observation of $B^+ \rightarrow \Xi_c^0 \Lambda_c^+$ and evidence for $B^0 \rightarrow \Xi_c^- \Lambda_c^+$ decays. Charge

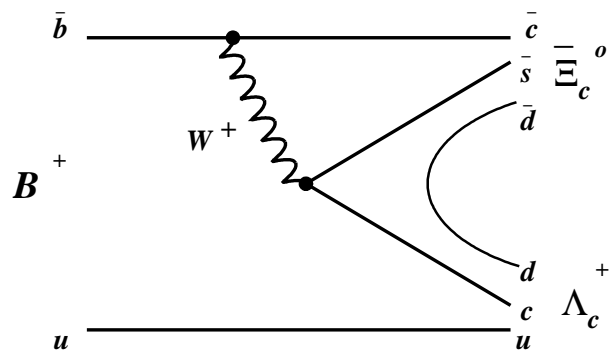


FIG. 1: The quark diagram for the $B^+ \rightarrow \Xi_c^0 \Lambda_c^+$ decay.

conjugation is implied here and throughout the paper. The analysis is performed using data collected with the Belle detector at the KEKB asymmetric-energy e^+e^- collider [12]. The data sample consists of 357 fb^{-1} collected at the $\Upsilon(4S)$ resonance, which corresponds to $386 \times 10^6 B\bar{B}$ pairs.

The Belle detector is a large-solid-angle magnetic spectrometer that consists of a silicon vertex detector (SVD), a 50-layer central drift chamber (CDC), an array of aerogel threshold Cherenkov counters (ACC), a barrel-like arrangement of time-of-flight scintillation counters (TOF), and an electromagnetic calorimeter (ECL) comprised of CsI(Tl) crystals located inside a superconducting solenoid coil that provides a 1.5 T magnetic field. An iron flux-return located outside of the coil is instrumented to detect K_L^0 mesons and to identify muons (KLM). The detector is described in detail elsewhere [13]. Two different inner detector configurations were used. For the first sample of 152 million $B\bar{B}$ pairs (Set I), a 2.0 cm radius beampipe and a 3-layer silicon vertex detector were used; for the latter 234 million $B\bar{B}$ pairs (Set II), a 1.5 cm ra-

dius beampipe, a 4-layer silicon detector and a small-cell inner drift chamber were used [14]. We use GEANT-based Monte Carlo (MC) simulation to model the response of the detector and determine the efficiency [15].

We select charged pions, kaons and protons that originate from the region $dr < 1$ cm, $|dz| < 4$ cm, where dr and dz are the distances of closest approach to the interaction point in the plane perpendicular to the beam axis ($r - \phi$ plane) and along the beam direction, respectively. Pions, kaons and protons are identified using a likelihood ratio method, which combines information from the TOF system and ACC counters with dE/dx measurements in the CDC [16].

In this analysis we reconstruct the following decay modes: $\Xi_c^0 \rightarrow \Xi^- \pi^+$ and $\Lambda K^- \pi^+$, $\Xi_c^+ \rightarrow \Xi^- \pi^+ \pi^+$, $\Lambda_c^+ \rightarrow p K^- \pi^+$, $\Xi^- \rightarrow \Lambda \pi^-$ and $\Lambda \rightarrow p \pi^-$. For $\Lambda \rightarrow p \pi^-$, we fit the p and π tracks to a common vertex and require an invariant mass in a ± 5 MeV/ c^2 interval around the Λ mass. The distance between the Λ decay vertex position and interaction point (IP) in the $r - \phi$ plane ($dr(\Lambda)$) is required to be greater than 0.05 cm and the angle α_Λ , between the Λ momentum vector and the vector pointing from the IP to the decay vertex, must satisfy $\cos \alpha_\Lambda > 0.995$ for the case of $\Xi_c^0 \rightarrow \Lambda K^- \pi^+$. We make no requirements on dr and $|dz|$ for tracks coming from $\Xi^- \rightarrow \Lambda \pi^-$ and $\Lambda \rightarrow p \pi^-$ decays. For $\Xi^- \rightarrow \Lambda \pi^-$, we fit the Λ trajectory and the π^- track to a common vertex and require a $\Lambda \pi^-$ invariant mass in a ± 5 MeV/ c^2 interval around the Ξ^- mass. We require that the distance between the Ξ^- decay vertex position and IP in the $r - \phi$ plane to be greater than 0.01 cm. For the Λ 's coming from Ξ^- in the decay $\Xi_c^0 \rightarrow \Xi^- \pi^+$ we apply the requirements, $dr(\Lambda) > 0.5$ cm and $\cos \alpha_\Lambda > 0.0$. For Λ_c^+ , Ξ_c^0 and Ξ_c^+ we use mass windows that are ± 15 MeV/ c^2 around their nominal values. We use a large sample of inclusive Λ , Ξ^- , $\Xi_c^{+/0}$ and Λ_c^+ signals to verify that their mass peaks are well described by two Gaussians, corresponding to the core and tail of the distribution. The signal mass windows that are used in this analysis correspond to approximately 4σ for the core and 2σ for the tail Gaussian. The MC studies of the inclusive Λ , Ξ^- , $\Xi_c^{+/0}$ and Λ_c^+ signals show agreement with data.

The B candidates (*i.e.* $\Xi_c \Lambda_c^+$ combinations) are identified by their center of mass (c.m.) energy difference, $\Delta E = \sum_i E_i - E_{\text{beam}}$, and their beam-energy constrained mass, $M_{bc} = \sqrt{E_{\text{beam}}^2 - (\sum_i \vec{p}_i)^2}$, where $E_{\text{beam}} = \sqrt{s}/2$ is the beam energy in the c.m. and \vec{p}_i and E_i are the three-momenta and energies of the B candidate's decay products. We accept B candidates with $M_{bc} > 5.2$ GeV/ c^2 and $|\Delta E| < 0.2$ GeV. To suppress the continuum background, we require the normalized Fox-Wolfram moment [17] R_2 to be less than 0.5. We apply $|\cos \theta_B| < 0.85$ for the Ξ_c^0 reconstruction in the $\Lambda K^- \pi^+$ mode, to suppress the combinatorial background. Here θ_B is the polar angle of the B -meson direction in the c.m.

The ΔE and M_{bc} distributions for the $B^+ \rightarrow \Xi_c^0 \Lambda_c^+$ candidates are shown in Figs. 2 (a) and (b), where the two Ξ_c^0 modes are combined. We require $M_{bc} > 5.272$ GeV/ c^2 ($|\Delta E| < 0.025$ GeV) for the ΔE (M_{bc}) projection [18]. The hatched histograms in Figs. 2 (a) and (b) show the sum of normalized Λ_c^+ and Ξ_c^0 mass sidebands [19] where no peaking structures are evident. The superimposed curves are the results of a simultaneous two-dimensional binned maximum likelihood fit to the both ΔE versus M_{bc} distributions (for the two Ξ_c^0 channels) with a common value of $\mathcal{B}(B^+ \rightarrow \Xi_c^0 \Lambda_c^+) \times \mathcal{B}(\Xi_c^0 \rightarrow \Xi^+ \pi^-) \times \mathcal{B}(\Lambda_c^+ \rightarrow p K^- \pi^+)$. For this fit, we constrain the ratio $\mathcal{B}(\Xi_c^0 \rightarrow \Lambda K^- \pi^+)/\mathcal{B}(\Xi_c^0 \rightarrow \Xi^- \pi^+)$ to the recent Belle measurement of $1.07 \pm 0.12 \pm 0.07$ [20]. To describe the signal we use Gaussians with means and widths fixed to the values obtained from MC. The backgrounds in ΔE and M_{bc} are parametrized by a first-order polynomial and an ARGUS function [21], respectively. The fit gives a statistical significance of 8.7σ for the signal, where the statistical significance is defined as $\sqrt{-2 \ln(L_0/L_{\text{max}})}$, where L_0 and L_{max} are the likelihoods with the signal fixed at zero and at the fitted value, respectively. The region $\Delta E < -0.08$ GeV is excluded from the fit to avoid possible contributions from $B^{+0} \rightarrow \Xi_c^0 \Lambda_c^+ \pi^{0/-}$ and $B^{0/+} \rightarrow \Xi_c^0 \Sigma_c^{0/+}, \Sigma_c^{0/+} \rightarrow \Lambda_c^+ \pi^{-/0}$ decays, where the pion is undetected. The same fitting procedure applied separately for the two Ξ_c^0 modes gives $12.4_{-3.3}^{+4.2}$ (6.8σ significance) and $16.9_{-4.0}^{+4.8}$ (5.9σ significance) events for $B^+ \rightarrow \Xi_c^0 \Lambda_c^+$ followed by $\Xi_c^0 \rightarrow \Xi^+ \pi^-$ and $B^+ \rightarrow \Xi_c^0 \Lambda_c^+$ followed by $\Xi_c^0 \rightarrow \bar{\Lambda} K^+ \pi^-$, respectively.

As a cross-check of the $B^+ \rightarrow \Xi_c^0 \Lambda_c^+$ signal, we select events in the B -signal region of $|\Delta E| < 0.025$ GeV and $M_{bc} > 5.272$ GeV/ c^2 for two Ξ_c^0 modes and examine the Λ_c^+ and Ξ_c^0 mass distributions (Fig. 2 (c) and (d)). For the Λ_c^+ (Ξ_c^0) distribution we require Ξ_c^0 (Λ_c^+) to be within ± 15 MeV/ c^2 of the nominal mass. We then fit each distribution with two Gaussians for the signal and a first-order polynomial to describe the background. The widths and means of the Gaussians are fixed to the values obtained from data as described above. The fitted signal yields of 32.6 ± 7.2 events for the Λ_c^+ and 29.4 ± 6.9 events for the Ξ_c^0 are in good agreement with the total signal yield for $B^+ \rightarrow \Xi_c^0 \Lambda_c^+$, including the two Ξ_c^0 decay modes.

The $B^0 \rightarrow \Xi_c^- \Lambda_c^+$ mode is an isospin partner of the $B^+ \rightarrow \Xi_c^0 \Lambda_c^+$ mode. Therefore their branching fractions are expected to be of the same order of magnitude. The ΔE and M_{bc} distributions for the $B^0 \rightarrow \Xi_c^- \Lambda_c^+$ candidates are shown in Figs. 3 (a) and (b). The superimposed curves are the results of a two-dimensional binned maximum likelihood fit to the ΔE versus M_{bc} distribution. The fit gives $8.3_{-2.5}^{+3.3}$ signal events. The signal significance is 3.8σ , taking into account the systematic uncertainty from the signal and background parameterization. The hatched histogram shows the sum of the normalized Λ_c^+ and Ξ_c^- mass sidebands. We apply the same procedure

TABLE I: Summary of the fit results, efficiencies, products of branching fractions and statistical significances. For the B^+ for two Ξ_c^0 modes the product of branching fractions is $\mathcal{B}(B^+ \rightarrow \Xi_c^0 \Lambda_c^+) \times \mathcal{B}(\Xi_c^0 \rightarrow \Xi^+ \pi^-)$ since for $\Xi_c^0 \rightarrow \bar{\Lambda} K^+ \pi^-$ we use the ratio $\mathcal{B}(\Xi_c^0 \rightarrow \Lambda K^- \pi^+)/\mathcal{B}(\Xi_c^0 \rightarrow \Xi^- \pi^+)$ mentioned in the text. The uncertainties in the products of the branching ratios are statistical, systematic and the uncertainty of the $\Lambda_c^+ \rightarrow p K^- \pi^+$ branching fraction.

Decay Mode	Yield	Efficiency(%)	Product of \mathcal{B} 's (10^{-5})	Significance
$B^+ \rightarrow \Xi_c^0 \Lambda_c^+, \Xi_c^0 \rightarrow \Xi^+ \pi^-$	$12.4^{+4.2}_{-3.3}$	1.14	$5.6^{+1.9}_{-1.5} \pm 1.1 \pm 1.5$	6.8σ
$B^+ \rightarrow \Xi_c^0 \Lambda_c^+, \Xi_c^0 \rightarrow \bar{\Lambda} K^+ \pi^-$	$16.9^{+4.8}_{-4.0}$	2.04	$4.0^{+1.1}_{-0.9} \pm 0.9 \pm 1.0$	5.9σ
$B^+ \rightarrow \Xi_c^0 \Lambda_c^+, \text{ simultaneous fit}$			$4.8^{+1.0}_{-0.9} \pm 1.1 \pm 1.2$	8.7σ
$B^0 \rightarrow \Xi_c^- \Lambda_c^+, \Xi_c^- \rightarrow \Xi^+ \pi^- \pi^-$	$8.3^{+3.3}_{-2.5}$	0.46	$9.3^{+3.7}_{-2.8} \pm 1.9 \pm 2.4$	3.8σ

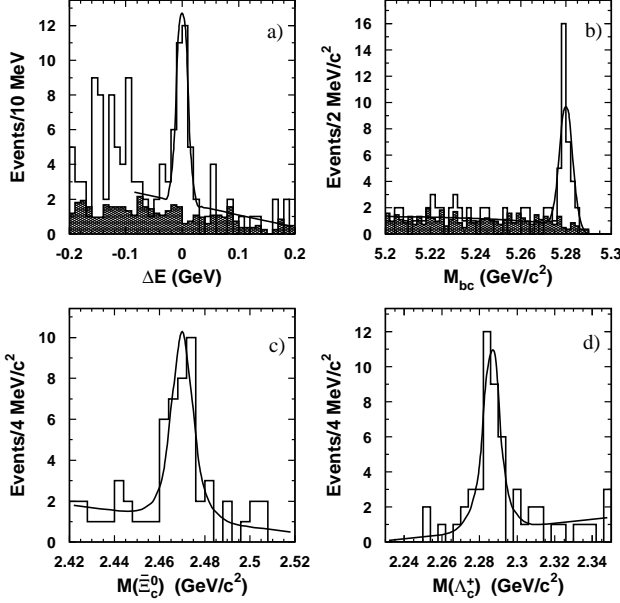


FIG. 2: a) and b): The ΔE (a) and M_{bc} (b) distributions for the $B^+ \rightarrow \Xi_c^0 \Lambda_c^+$ candidates. The hatched histograms show the combined Ξ_c^0 and Λ_c^+ mass sidebands normalized to the signal region. The excess around $\Delta E = -0.150$ GeV may be due to the contributions from $B^{+/\bar{0}} \rightarrow \Xi_c^0 \Lambda_c^+ \pi^{0/-}$ and $B^{0/+} \rightarrow \Xi_c^0 \Sigma_c^{0/+}, \Sigma_c^{0/+} \rightarrow \Lambda_c^+ \pi^{-/0}$ decays, where the pion is undetected. Therefore, we exclude this region from the fit. c) and d): The Ξ_c^0 (c) and Λ_c^+ (d) mass distributions for the $B^+ \rightarrow \Xi_c^0 \Lambda_c^+$ candidates taken from the B-signal region of $|\Delta E| < 0.025$ GeV and $M_{bc} > 5.272$ GeV/ c^2 . For the Ξ_c^0 (Λ_c^+) distribution we require Λ_c^+ (Ξ_c^0) to be within ± 15 MeV/ c^2 of the nominal mass. The overlaid curves are the fit results (see the text).

used for $B^+ \rightarrow \Xi_c^0 \Lambda_c^+$ to check the Λ_c^+ and Ξ_c^- signals as shown in Figs. 3 (c) and (d). The fit gives 9.0 ± 3.0 events for the Λ_c^+ and 8.4 ± 2.8 events for the Ξ_c^- . Both are in agreement with the $B^0 \rightarrow \Xi_c^- \Lambda_c^+$ signal yield.

Table I summarizes the results of the fits for the B^+ and B^0 decays, the reconstruction efficiencies including the $\mathcal{B}(\Lambda \rightarrow p \pi^-)$, statistical significance of the signals and extracted products of branching fractions. Here we

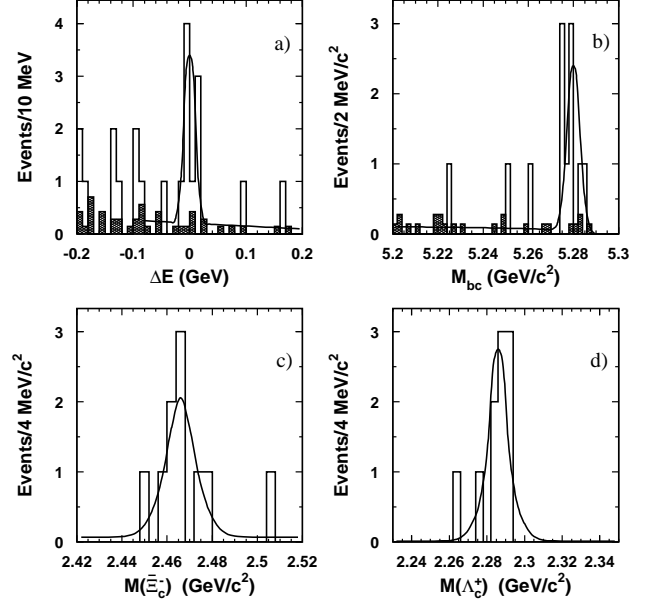


FIG. 3: a) and b): The ΔE (a) and M_{bc} (b) distributions for the $B^0 \rightarrow \Xi_c^- \Lambda_c^+$ candidates. The hatched histograms show the combined Ξ_c^- and Λ_c^+ mass sidebands normalized to the signal region. c) and d): The Ξ_c^- (c) and Λ_c^+ (d) mass distributions for the $B^0 \rightarrow \Xi_c^- \Lambda_c^+$ candidates taken from the B-signal region of $|\Delta E| < 0.025$ GeV and $M_{bc} > 5.272$ GeV/ c^2 . For the Ξ_c^- (Λ_c^+) distribution we require Λ_c^+ (Ξ_c^-) to be within ± 15 MeV/ c^2 of the nominal mass. The overlaid curves are the fit results (see the text).

use $\mathcal{B}(\Lambda_c^+ \rightarrow p K^- \pi^+) = (5.0 \pm 1.3)\%$ [8] and assume equal fractions of charged and neutral B mesons produced in $\Upsilon(4S)$ decays.

The major sources of systematic error are the uncertainties in the tracking efficiency of 7% (1% per track), 11% in charged particle identification efficiency (1% for pion, 2% for kaon and 3% for proton), 5% in Λ finding, 6% in efficiency estimation due to MC statistics, 10% in the signal and background parameterization, and 13% in $\mathcal{B}(\Xi_c^0 \rightarrow \Lambda K^- \pi^+)/\mathcal{B}(\Xi_c^0 \rightarrow \Xi^- \pi^+)$. Added in quadrature, these correspond to a total systematic error of 23% for $B^+ \rightarrow \Xi_c^0 \Lambda_c^+$ and 20% for $B^0 \rightarrow \Xi_c^- \Lambda_c^+$.

In summary, we report the first observation of the $B^+ \rightarrow \Xi_c^0 \Lambda_c^+$ decay mode and the first evidence for the $B^0 \rightarrow \Xi_c^- \Lambda_c^+$ decay mode. The products of branching fractions $\mathcal{B}(B^+ \rightarrow \Xi_c^0 \Lambda_c^+) \times \mathcal{B}(\Xi_c^0 \rightarrow \Xi^+ \pi^-) = (4.8_{-0.9}^{+1.0} \pm 1.1 \pm 1.2) \times 10^{-5}$ and $\mathcal{B}(B^0 \rightarrow \Xi_c^- \Lambda_c^+) \times \mathcal{B}(\Xi_c^- \rightarrow \Xi^+ \pi^- \pi^-) = (9.3_{-2.8}^{+3.7} \pm 1.9 \pm 2.4) \times 10^{-5}$ are measured with 8.7σ and 3.8σ significance, respectively. These results and Belle's recent observation of $B \rightarrow \Lambda_c^+ \bar{\Lambda}_c^- K$ [7] decays are the first examples of B decays into two charmed baryons. The branching fraction obtained for $B^+ \rightarrow \Xi_c^0 \Lambda_c^+$ together with the theoretical predictions for $\mathcal{B}(\Xi_c^0 \rightarrow \Xi^- \pi^+)$ of $\sim (0.9 - 2)\%$ [22] result in $\mathcal{B}(B^+ \rightarrow \Xi_c^0 \Lambda_c^+) \sim (2.4 - 5.3) \times 10^{-3}$. This can be compared with the theoretical prediction of 10^{-3} [11]. On the other hand, the Belle measurement of $\mathcal{B}(\bar{B}^0 \rightarrow \Lambda_c^+ \bar{p}) = (2.19_{-0.49}^{+0.56} \pm 0.32 \pm 0.57) \times 10^{-5}$ [23] is much smaller than their prediction of 4×10^{-4} [11]. The very large ratio of ~ 100 for $\mathcal{B}(B \rightarrow \Xi_c^0 \Lambda_c^+)/\mathcal{B}(\bar{B}^0 \rightarrow \Lambda_c^+ \bar{p})$ disagrees with the naive expectation that the branching fractions for two-body baryonic B decays proceeding via $b \rightarrow c\bar{c}s$ and $b \rightarrow c\bar{u}d$ transitions should be of the same order [11].

We thank the KEKB group for excellent operation of the accelerator, the KEK cryogenics group for efficient solenoid operations, and the KEK computer group and the NII for valuable computing and Super-SINET network support. We acknowledge support from MEXT and JSPS (Japan); ARC and DEST (Australia); NSFC (contract No. 10175071, China); DST (India); the BK21 program of MOEHRD, and the CHEP SRC and BR (grant No. R01-2005-000-10089-0) programs of KOSEF (Korea); KBN (contract No. 2P03B 01324, Poland); MIST (Russia); MHEST (Slovenia); SNSF (Switzerland); NSC and MOE (Taiwan); and DOE (USA).

[1] Belle Collaboration, K. Abe *et al.*, Phys. Rev. Lett. **89**, 151802 (2002).
[2] Belle Collaboration, N. Gabyshev, H. Kichimi *et al.*, Phys. Rev. D **66**, 091102(R) (2002).
[3] Belle Collaboration, Y.-J. Lee, M.-Z. Wang *et al.*, Phys. Rev. Lett. **93**, 211801 (2004); M.-Z. Wang, Y.-J. Lee, *et al.* (Belle Collaboration), Phys. Rev. Lett. **90**, 201802 (2003); Belle Collaboration, K. Abe *et al.*, Phys. Rev. Lett. **88**, 181803 (2002).
[4] H. Kichimi, Nucl. Phys. B Proc. Suppl. **142**, 197 (2005).
[5] W. S. Hou and A. Soni, Phys. Rev. Lett. **86**, 4247 (2001);

C. K. Chua, W. S. Hou and S. Y. Tsai, Phys. Lett. B **528**, 233 (2002).
[6] Belle Collaboration, Q. L. Xie *et al.*, Phys. Rev. D **72**, 051105(R) (2005).
[7] Belle Collaboration, K. Abe *et al.*, hep-ex/0508015.
[8] S. Eidelman *et al.*, Review of Particle Physics, Phys. Lett. B **592**, 1 (2004).
[9] BaBar Collaboration, B. Aubert *et al.*, Phys. Rev. D **70**, 091106 (2004).
[10] I. Dunietz, P. Cooper, A. Falk and M. Wise, Phys. Rev. Lett. **73**, 1075 (1994).
[11] V. L. Chernyak and I. R. Zhitnitsky, Nucl. Phys B **345**, 137 (1990).
[12] S. Kurokawa and E. Kikutani, Nucl. Instrum. Methods Phys. Res., Sect. A **499**, 1 (2003), and other papers included in this volume.
[13] Belle Collaboration, A. Abashian *et al.*, Nucl. Instrum. Methods Phys. Res., Sect. A **479**, 117 (2002).
[14] Belle SVD2 Group, Y. Ushiroda Nucl. Instrum. Methods Phys. Res., Sect. A **511**, 6 (2003).
[15] R. Brune *et al.*, GEANT 3.21, CERN DD/EE/84-1, 1984.
[16] Charged kaons are required to satisfy $\mathcal{L}(K)/(\mathcal{L}(K) + \mathcal{L}(\pi)) > 0.6$ and $\mathcal{L}(K)/(\mathcal{L}(K) + \mathcal{L}(p)) > 0.6$. Charged pions are required to satisfy $\mathcal{L}(\pi)/(\mathcal{L}(K) + \mathcal{L}(\pi)) > 0.1$ and $\mathcal{L}(\pi)/(\mathcal{L}(\pi) + \mathcal{L}(p)) > 0.1$. Protons are required to satisfy $\mathcal{L}(p)/(\mathcal{L}(K) + \mathcal{L}(p)) > 0.6$ and $\mathcal{L}(p)/(\mathcal{L}(\pi) + \mathcal{L}(p)) > 0.6$. Here $\mathcal{L}(K/\pi/p)$ is the particle identification likelihood for the $K/\pi/p$ hypotheses. The above requirements have efficiencies of more than 95% for pions, kaons and protons, respectively, from $B \rightarrow \Xi_c \Lambda_c^+$ decays. The probability for each particle species to be misidentified as one of the other two is less than 5%.
[17] G. Fox and S. Wolfram, Phys. Rev. Lett. **41**, 1581 (1978).
[18] We found that after applying all the selection requirements, there are no multiple entries in the M_{bc} and ΔE distributions.
[19] For the Ξ_c^0 , the sidebands are determined as follows: $2.4 < M(\Xi_c^0) < 2.44$ GeV/ c^2 or $2.5 < M(\Xi_c^0) < 2.54$ GeV/ c^2 . For the Λ_c^+ the sidebands are determined as follows: $2.22 < M(\Lambda_c^+) < 2.26$ GeV/ c^2 or $2.32 < M(\Lambda_c^+) < 2.36$ GeV/ c^2 .
[20] Belle Collaboration, T. Lesiak *et al.*, Phys. Lett. B **605**, 237 (2005), Erratum **617**, 198 (2005).
[21] ARGUS Collaboration, H. Albrecht *et al.*, Phys. Lett. B **241**, 278 (1990).
[22] B. Desplanques, J. F. Donoghue and B. R. Holstein, Annals Phys. **124**, 449 (1980); P. Zenczykowski, Phys. Rev. D **40**, 2290 (1989); P. Zenczykowski, Phys. Rev. D **50**, 402 (1994).
[23] Belle Collaboration, N. Gabyshev, H. Kichimi, *et al.*, Phys. Rev. Lett. **90**, 121802 (2003).